Human adenovirus infection causes the cellular MKRN1 E3 ubiquitin ligase degradation involving the viral core protein pVII

Raviteja Inturi[a], Kwangchol Mun[a], Katrin Singethan[b], Sabrina Schreiner[b] and Tanel Punga[a]#

Department of Medical Biochemistry and Microbiology, Uppsala University, Uppsala, Sweden[a]; Institut für Virologie, Technische Universität München/Helmholtz Zentrum München, München, Germany[b]

Running Head: Inactivation of the MKRN1 protein by human adenovirus

#Address correspondence to Tanel Punga, Tanel.Punga@imbim.uu.se

Abstract word count: 223

Text word count: 5340

ABSTRACT

Human adenoviruses (HAdVs) are common human pathogens encoding a highly abundant histone-like core protein VII, which is involved in nuclear delivery and protection of viral DNA as well as in sequestering immune danger signals in infected cells. The molecular details of how protein VII acts as a multifunctional protein have remained to a large extent enigmatic. Here we report the identification of several cellular proteins interacting with the precursor pVII protein. We show that the cellular E3 ubiquitin ligase MKRN1 is a novel precursor pVII interacting protein in HAdV-C5-infected cells. Surprisingly, the endogenous MKRN1 protein underwent proteasomal degradation during the late phase of HAdV-C5 infection in various human cell lines. The MKRN1 protein degradation occurred independently of the HAdV E1B55K and E4orf6 proteins. We provide experimental evidence that the precursor pVII protein binding enhances MKRN1 self-ubiquitination, whereas the processed mature VII protein is deficient in this function. Based on these data, we propose that the pVII protein binding promotes MKRN1 self-ubiquitination followed by proteasomal degradation of the MKRN1 protein in HAdV-C5-infected cells. In addition, we show that measles virus and vesicular stomatitis virus infections reduce the MKRN1 protein accumulation in the recipient cells. Taken together, our results expand the functional repertoire of the HAdV-C5 precursor pVII protein in lytic virus infection and highlight MKRN1 as a potential common target during different virus infections.

44 **IMPORTANCE**

45 Human adenoviruses (HAdVs) are common pathogens causing a wide range of diseases.
46 To achieve pathogenicity HAdVs have to counteract a variety of host cell antiviral
47 defense systems, which would otherwise hamper virus replication. In this study, we show
48 that the HAdV-C5 histone-like core protein pVII binds to and promotes self-
49 ubiquitination of a cellular E3 ubiquitin ligase named as MKRN1. This mutual
50 interaction between the pVII and MKRN1 proteins may prime MKRN1 for proteasomal
51 degradation because the MKRN1 protein is efficiently degraded during the late phase of
52 HAdV-C5 infection. Since the MKRN1 protein accumulation is also reduced in measles
53 virus and vesicular stomatitis virus infected cells, our results signify the general strategy
54 of viruses to target MKRN1.
55
56

INTRODUCTION

Human adenoviruses (HAdVs) are common pathogens and their infections cause a wide range of diseases including respiratory illness, keratoconjunctivitis and gastroenteritis (1, 2). HAdVs are non-enveloped viruses with a linear double-stranded DNA genome embedded in a protective viral core structure. Inside the core, HAdV DNA associates with the viral proteins V, VII, Mu, terminal protein, and DNA-dependent adenovirus proteinase (Avp) (3). Protein VII is expressed during the late phase of infection and it accumulates as a precursor polypeptide, designated as the pVII protein (4). The precursor pVII protein undergoes site-specific Avp-dependent cleavage to form the mature VII protein during the final steps of virus maturation (5-9). This proteolytic cleavage step assures proper condensation of viral DNA and proteins within the HAdV core (10, 11). The Avp cleavage may also control protein stability, as compared to precursor pVII, mature VII is resistant to proteasomal degradation by cellular Cullin-3-based E3 ubiquitin ligase complexes (12).

Due to its histone-like characteristics, the mature VII protein is able to assemble viral DNA into nucleosome-like structures (11, 13-16). Although protein VII is not required to condense viral DNA within the capsid, lack of it blocks productive virus infection (17). Several functions have been assigned to protein VII due to its interaction with DNA. The mature VII promotes nuclear import of viral DNA (18-20) and protects incoming viral DNA from the cellular DNA damage response (21). Protein VII can also introduce changes into virus genome structure. This involves gradual loss of the mature VII protein from virus DNA during the transition from the early to the late phase of infection. Here, the reduced VII binding correlates with increased nucleosomal histone

accumulation on viral DNA (22, 23). Protein VII can also recruit cellular template activating factor TAF-1β (also known as SET) to remodel the virus genome and to increase accessibility to transcription factors (24-26). Since protein VII interacts with DNA it can have both negative and positive effects on target gene expression (22, 27). In addition to viral DNA, the mature protein VII also associates with host cell chromatin. By binding to cellular nucleosomes, mature VII alters the cellular HMGB1 and HMGB2 protein functions on the host cell chromatin and thereby suppresses cellular inflammatory signaling (28). Binding of mature VII to cellular chromatin can also inhibit the DNA damage response on the host genome (29).

Covalent attachment of the ubiquitin moiety by the E3 ubiquitin ligases to substrate proteins can lead to proteolytic degradation via the ubiquitin-proteasome system (UPS) (30). Viruses, such as HAdV, often target UPS to achieve efficient replication in host cells (reviewed in (31-33)). This is exemplified by HAdV E1B55K/E4orf6 protein complexes, which by recruiting Cullin-based E3 ubiquitin ligases, promote proteasomal degradation of the cellular p53, Mre11, DNA ligase IV, integrin α3, Tip60, ATRX, Daxx and SPOC1 proteins (34-40).

The Makorin ring finger protein 1 (MKRN1) gene was first reported as an intron-containing source gene for the Makorin ring finger (MKRN) gene family. This conserved protein contains several zinc finger motifs and a single RING finger domain (41). MKRN1 functions as an E3 ubiquitin ligase since it contains a functional RING finger domain at the C-terminus of the protein (42). Several cellular proteins, including hTERT, p53, p21, PPARγ, p14ARF, FADD, PTEN, are known substrates for MKRN1-mediated ubiquitination and proteasomal degradation (42-47). Also viral proteins, such as West

Nile virus (WNV) and porcine circovirus type 2 (PCV2) capsid proteins, interact with MKRN1 (48, 49). Only WNV capsid protein (WNVCp) has been shown to be ubiquitinated and degraded by the proteasome in a MKRN1-dependent manner (48). The MKRN1 protein has also been characterized as an RNA-binding protein with potential to regulate RNA metabolism in mouse embryonic stem cells (50). Further, MKRN1 can repress transcription on different cellular promoters independently of its described E3 ligase activity (46, 51).

Even though protein VII has been extensively characterized as a virus DNA-binding protein, not much is known about its interactions with cellular proteins. Considering its essential role during productive infection (17), it is reasonable to assume that protein VII interacts with a variety of cellular proteins. This study was undertaken to identify novel precursor pVII interacting proteins and to elucidate the functional consequences of these interactions.

RESULTS

Identification of precursor pVII interacting proteins

To identify cellular proteins specifically interacting with HAdV-C5 precursor pVII protein, we performed a yeast two-hybrid (Y2H) screening experiment. The precursor pVII protein (hereafter referred to as pVII(wt)) was used as the bait to screen the human lung cancer cell line cDNA library. Sequencing of the cDNA clones identified 13 potential proteins interacting with the precursor pVII protein (Table 1). The identified proteins were further grouped based on their Predicted Biological Score (PBS, see

Materials and Methods). The proteins having the highest number of clones and the best PBS score were C1QBP, SET, HMGB2, HMGB3. In addition, the Y2H screen recovered clones with lower PBS scores, such as SETSIP, ZNF622, CHD3, MKRN1, BAZ1A, CTPS1, RACK1. The specificity of our Y2H screen was strengthened by the observation that the SET, HMGB2 and HMGB3 proteins have been previously shown to bind the mature VII protein (hereafter referred to as pVII(Δ24)) in HAdV-infected cells (28, 52). To validate the Y2H screen results, we performed a proximity ligation assay (PLA) in HeLa cells expressing the precursor pVII-Flag protein (hereafter referred to as pVII(wt)-Flag) after doxycycline treatment. PLA was performed with the antibodies against some of the identified proteins (Table 1) and with an anti-Flag-antibody to detect protein-protein interactions in cells. All the tested proteins showed detectable proximity ligation in the pVII(wt)-Flag protein expressing cells (Fig. 1). Further quantification confirmed that proximity ligation of the HMGB2, C1QBP, MKRN1, SET, BAZ1A, CHD3 proteins with pVII(wt)-Flag protein was above the background signal obtained with an irrelevant antibody in the control reaction.

Since the pVII(wt) protein stability can be controlled by UPS (12), we concentrated our efforts on the identified E3 ubiquitin ligase MKRN1 and its interference with the pVII(wt) protein.

The precursor pVII protein interacts with MKRN1 in HAdV-C5-infected cells

To study whether MKRN1 interacts with pVII(wt) during HAdV-C5 infection, we generated a replication-competent HAdV-C5 virus expressing Flag-epitope containing pVII protein (hereafter referred to as HAdV-pVII-Flag). This virus was used to infect

H1299 cells followed by immunoprecipitation of the pVII(wt)-Flag protein 20 h post infection (hpi). The results confirmed that pVII(wt)-Flag interacts with the endogenous MKRN1 protein in virus-infected cells and that this interaction was enhanced in the presence of proteasome inhibitor MG132 (Fig. 2A, lanes 4 to 6). To show the assay specificity, we confirmed that pVII(wt)-Flag interacted with HMGB2, a previously established protein VII interactor (28) (Fig. 2A, WB:HMGB2). In contrast, an abundant HAdV-C5 early protein, E1A, did not show detectable binding to the pVII-Flag protein in our experimental system (Fig. 2A, WB:E1A). Both precursor pVII (pVII(wt)) and mature VII (pVII(Δ24)) (12) proteins are present in HAdV-C5-infected cells (53). Mature VII is generated from precursor pVII after Avp proteolytic cleavage of the propeptide module (7, 8). To study if the propeptide module (amino acids 1-24 in HAdV-C5) influences the precursor pVII protein binding to MKRN1, we performed co-immunoprecipitation experiments with H1299 cell lysates expressing the pVII(wt)-Flag or pVII(Δ24)-Flag proteins in presence of HA-MKRN1(wt). As shown in Fig. 2B, the lack of propeptide sequence in pVII(Δ24) reduced the protein binding to HA-MKRN1(wt) (lanes 5 and 6). A similar result was observed with the GST pull-down experiment where GST-pVII(Δ24) showed reduced binding to Flag-MKRN1 when compared to GST-pVII(wt) (Fig. 2C). In order to identify which region(s) of the MKRN1 protein interact with pVII, different HA-tagged MKRN1 deletion mutant proteins were constructed (Fig. 2D). The GST pull-down experiment with H1299 cell lysates expressing the HA-MKRN1 proteins revealed that both N-terminal (amino acids 1-267) and C-terminal (112-482) MKRN1 regions were able to bind to GST-pVII(wt) (Fig. 2E). Since the HA-MKRN1(112-267) protein was

171 deficient in binding to pVII (Fig. 2E, lane 11), it is likely that HA-MKRN1 amino acid
172 regions 1-111 and 268-482 provide interaction surface for the pVII(wt) protein.
173
174 **The MKRN1 protein undergoes proteasomal degradation in HAdV-C5-infected cells**
175 Since HAdV infections cause proteasomal degradation of several host proteins (reviewed
176 in (31-33)), it became of interest to evaluate the steady state level of the endogenous
177 MKRN1 protein in HAdV-C5-infected cells. H1299 cells were infected with HAdV-C5
178 and the endogenous MKRN1 protein was monitored during a 48 h infection time course.
179 The MKRN1 protein was undetectable from 20 hpi and onwards, overlapping with virus
180 capsid protein accumulation in the infected H1299 cells (Fig. 3A). To establish if the
181 MKRN1 protein disappearance was due to its proteasomal degradation, HAdV-C5-
182 infected H1299 cells were treated with MG132. The MKRN1 protein levels were restored
183 in the MG132 treated cells (Fig. 3B, lanes 3 and 4), indicating that the protein undergoes
184 proteasomal degradation in HAdV-C5-infected cells. This is further supported by the
185 observation whereby MKRN1 mRNA accumulation was not affected in infected H1299
186 cells (Fig. 3C). To test if the observed MKRN1 disappearance correlated with
187 accumulation of the pVII protein during infection, H1299 cells were infected with the
188 HAdV-pVII-Flag virus. As shown in Fig. 3D, expression of pVII from 16 hpi and
189 onwards correlated with reduced accumulation of the MKRN1 protein. MKRN1
190 disappearance was not H1299 cell line specific since similar effect was observed in
191 HAdV-C5-infected A549, U2OS and HEK293 cell lines (Fig. 3E). Taken together, our
192 results indicate that MKRN1 undergoes proteasomal degradation during the late phase of
193 infection in various HAdV-C5-infected cell lines.

The MKRN1 protein degradation is independent of the E1B55K and E4orf6 proteins

HAdVs encode the E1B55K and E4orf6 proteins, which by binding to Cullin-based E3 ubiquitin ligases induce proteasomal degradation of cellular proteins in infected cells. To investigate whether MKRN1 degradation is dependent on the E1B55K and E4orf6 proteins, Flag-tagged versions of both proteins were transiently overexpressed in H1299 cells. As shown in Fig. 4A, endogenous MKRN1 was not affected by expression of the Flag-E1B55K and/or Flag-E4orf6 proteins. In the same experiment, a well-known E1B55K/E4orf6 target protein, Mre11 (40), was downregulated (Fig. 4A, lanes 4 and 8, see also the quantification). To further demonstrate that proteasomal degradation of MKRN1 occurs independently of the E1B55K/E4orf6 complex, H1299 cells were infected with wild-type HAdV-C5 and E1B55K-deleted, dl1520, virus (54). The MKRN1 protein levels were reduced by both virus infections, whereas the Mre11 protein was affected only in wild-type virus-infected cells (Fig. 4B). Taken together, our data suggest that proteasomal degradation of MKRN1 in HAdV-infected cells occurs independently of the E1B55K/E4orf6 protein complex.

The pVII(wt) protein enhances MKRN1 protein self-ubiquitination

The MKRN1 protein binds to the substrate proteins via the C-terminal RING finger domain to promote target protein ubiquitination and proteasomal degradation (42, 48). In addition, MKRN1 undergoes self-ubiquitination and proteasomal degradation, which may control its activity in cells (42, 55). Since pVII(wt) interacts with MKRN1 via the RING

finger domain (Fig. 2E), our initial logical follow-up was to test if the pVII(wt) protein was ubiquitinated in an MKRN1-dependent manner. Despite several attempts we were unable to detect MKRN1-dependent pVII(wt) ubiquitination (data not shown). The observation that pVII(wt) binds also to N-terminal part of MKRN1 (Fig. 2E) urged us to test whether this viral protein has any impact on the MKRN1 E3 ubiquitin ligase activity. Expression of the precursor pVII(wt)-Flag protein enhanced MKRN1 ubiquitination in His-ubiquitin expressing H1299 cells when analyzed with nickel pull-down experiment (Fig. 5A, lanes 2 to 3). Enhanced MKRN1 ubiquitination was specific to the pVII(wt)-Flag protein since basal MKRN1 ubiquitination remained the same in cells expressing the mature VII (pVII(Δ24)) protein (Fig. 5A, lanes 2 and 4). The inability of pVII(Δ24) to enhance MKRN1 ubiquitination is probably due to reduced binding of the pVII(Δ24) protein to MKRN1 (Figs. 2B and 2C). Further, the specificity of experiment was confirmed by the lack of ubiquitination in cells expressing the MKRN1(1-267) protein (Fig. 2D), which lacks the RING finger domain (Fig. 5A, lanes 5-8). Previous studies have shown that mutation of the histidine residue at position 307 (H307E) in the RING finger domain (Fig. 2D) blocks MKRN1 ability to ubiquitinate the substrate proteins (42, 46). The MKRN1(H307E) protein itself was ubiquitinated in our *in vivo* ubiquitination experiment in H1299 cells (Fig. 5B, lanes 3 and 7), suggesting that MKRN1(H307E) can serve as a substrate for ubiquitination. In contrast to HA-MKRN1(wt) (Fig. 5B, lanes 3 to 5), ubiquitination of the HA-MKRN1(H307E) protein was not enhanced by the pVII(wt)-Flag protein (Fig. 5B, lanes 7 to 9). This discrepancy was not due to different affinity of the MKRN1 proteins, as both HA-MKRN1(wt) and HA-MKRN1(H307E) bound equally well to pVII(wt)-Flag (Fig. 5C). The observation that MKRN1(H307E) was ubiquitinated

in our experiments urged us to further study the details of this particular mutation. We performed *in vitro* ubiquitination experiments with the purified E1 (His-UbE1), E2 (His-UbcH5a) and E3 (GST-MKRN1) proteins, which revealed that the MKRN1(H307E) protein is defective in self-ubiquitination (Fig. 5D, lanes 2 and 4). Since the pVII(wt) protein did not promote MKRN1(H307E) self-ubiquitination (Fig. 5B), we hypothesized that this mutant protein might be more stable in HAdV-C5-infected cells when compared to the wild-type protein. To test this hypothesis, we infected H1299 cells expressing either the HA-MKRN1(wt) or HA-MKRN1(H307E) protein with HAdV-pVII-Flag virus and blocked *de novo* protein synthesis with cycloheximide. As shown in Fig. 5E, the HA-MKRN1(wt) protein showed faster decay in the presence of cycloheximide compared to the HA-MKRN1(H307E) protein suggesting that the latter is resistant to proteasomal degradation in virus-infected H1299 cells. Collectively, our data indicate that pVII(wt), but not pVII(Δ24), enhances the MKRN1 protein self-ubiquitination.

Downregulation of MKRN1 is not limited to HAdV-C5 infection

Considering the effective elimination of MKRN1 in HAdV-C5-infected cells (Fig. 3), we hypothesized that MKRN1 might also be affected in cells infected with other pathogenic viruses. Therefore, we analyzed MKRN1 accumulation in permissive cells infected with HIV-1 (human immunodeficiency virus type 1), HCV (hepatitis C virus), MV (measles virus), VSV (vesicular stomatitis virus) and HBV (hepatitis B virus). The MKRN1 protein levels were reduced in MV- and VSV-infected cells, whereas the HIV-1, HCV and HBV infections did not considerably affect the MKRN1 protein levels (Fig. 6).

DISCUSSION

The HAdV mature VII protein has long been considered as a virus genome organizing factor (14). Although mature VII is not required to condense DNA within the capsid, it is essential for productive infection (17). The present study along with the recent elegant reports from Weitzman (28, 29) and Hearing laboratories (17), are the latest progressive attempts to elucidate the important functions of pVII protein in HAdV-infected cells.

In this report, we aimed to identify novel precursor pVII(wt) interacting proteins and to relate the identified interactors with yet uncharacterized functions of the pVII protein. We found that the pVII(wt) protein interacts with the CHD3 and BAZ1A proteins (Table 1 and Fig. 1), which are both involved in chromatin remodeling (56, 57). Considering the reported activities of the protein VII on gene expression (22, 27) and chromatin structure regulation (13, 15, 28), it is theoretically possible that pVII(wt) interaction with the CHD3 and BAZ1A proteins is needed to achieve optimal pVII-dependent chromatin remodeling in HAdV-infected cells. In addition, we identified two other chromatin structure regulating proteins, HMGB2 and HMGB3, as the pVII(wt) interacting proteins. This finding is in line with a recent report where the mature protein VII was shown to interact with the HMGB1, HMGB2 and HMGB3 proteins in A549 cells (28). Even though the mature VII impacts on antiviral responses by altering the HMGB1 and HMGB2 protein functions on the host cell chromatin, the functional impact of the pVII(wt) protein on HMGB3 remains to be tested.

One of the identified pVII(wt) interacting proteins in the Y2H screen was the E3 ubiquitin ligase MKRN1 (Table 1). Since we have previously shown that the precursor

pVII protein is targeted for proteasomal degradation (12), we hypothesized that MKRN1 might be the E3 ubiquitin ligase mediating pVII(wt) ubiquitination and its subsequent proteasomal degradation. Even though MKRN1 transient overexpression reduced pVII(wt) protein levels in a proteasome-dependent manner, we were unable to confirm that the pVII(wt) protein was directly ubiquitinated by MKRN1 (data not shown). Instead, our detailed analysis revealed that MKRN1 undergoes proteasomal degradation during the late phase of infection in various human cell lines (Fig. 3). In this regard, MKRN1 degradation in HAdV-C5-infected cells is unusual as it does not rely on the E1B55K and E4orf6 proteins (Fig. 4), which are well-characterized viral proteins targeting multiple cellular proteins for proteasomal degradation in HAdV-infected cells (31-33). Based on our protein-protein interaction experiments and observation that MKRN1 degradation correlated with onset of the HAdV late protein accumulation (Figs. 2 and 3), we hypothesized that the pVII(wt) protein might be involved in MKRN1 stability regulation. Previous studies have revealed that MKRN1 interacts with its target proteins, such as p53 and WNVCp, via the C-terminal RING finger domain to assure substrate protein ubiquitination and subsequent proteasomal degradation (46, 48). Our observation that pVII(wt) interacts with both MKRN1 N- and C-terminal regions suggested that pVII(wt) interference with MKRN1 may not follow a typical enzyme-substrate interaction leading to a substrate protein, such as pVII(wt), ubiquitination and degradation. This was supported by the observation that the precursor pVII protein enhanced MKRN1 self-ubiquitination, whereas the mature VII, which showed reduced binding to MKRN1, was deficient in this function (Figs. 5A and 5B). Therefore, we propose a model whereby during the late phase of infection the precursor pVII protein

saturates both the N- and C-terminal binding sites on MKRN1, which in turn leads to MKRN1 self-ubiquitination. This dual binding mode can be due to the increased pVII(wt) protein concentration during the late phase of infection. Alternatively, since the pVII protein is extensively modified by phosphorylation and acetylation (28, 58), it is possible that these post-translational modifications increase pVII(wt) affinity towards MKRN1. Our model suggests that precursor pVII may display separate functions from mature VII. This novel function assigned to precursor pVII may explain why the cleavage of the propeptide module occurs only during the final steps of virus particle maturation. Hypothetically, early cleavage of the precursor pVII to mature VII protein will not cause MKRN1 proteasomal degradation as the mature VII is deficient in promoting MKRN1 self-ubiquitination. Although the precursor pVII induces MKRN1 self-ubiquitination, expression of pVII(wt) alone, outside of the virus-infection context, was not sufficient to cause MKRN1 proteasomal degradation (data not shown). This observation implies that even though the precursor pVII protein enhances MKRN1 self-ubiquitination, there is a need for an additional, yet-unknown factor in HAdV-C5-infected cells to achieve MKRN1 proteasomal degradation.

We also found that two other pathogenic viruses, MV and VSV, affected MKRN1 protein accumulation in their respective recipient cells (Fig. 6). Three different virus infections (HAdV-C5, MV, VSV) downregulate the MKRN1 protein accumulation (present study) and at least two other viruses (WNV, PCV2) encode for the proteins interacting with MKRN1 (48, 49). Further, the observation that MKRN3 restricts HIV-1 infection in human cells may indicate the involvement of different MKRN gene family members in controlling virus infections (59). This broad targeting raises an important

question why different viruses impede MKRN1 functions. It is theoretically possible that downregulation of the MKRN1 protein is beneficial for optimal virus growth since MKRN1 may affect viral protein ubiquitination, gene transcription and RNA metabolism. Further studies are needed to reveal the exact role of the MKRN1 and its family members in various virus infections.

In conclusion, our novel findings expand the functional repertoire of the precursor pVII protein in lytic HAdV-C5 infection and highlight MKRN1 as a common target protein during different virus infections.

MATERIALS AND METHODS

Plasmids, siRNAs and cell lines

Human MKRN1 (NM_013446) GenEZ ORF Clone (GenScript, Inc) was cloned into pcDNA3.1-HA and pcDNA3.1-Flag plasmids to express HA- and Flag-tagged MKRN1 proteins. In the same plasmid background, MKRN1 point mutant (H307E) and deletion mutants (1-267, 112-267, 112-482) were generated using QuikChange Lightning Site-Directed Mutagenesis Kit (Agilent Technologies) and PCR-mediated DNA deletion, respectively. To express the GST-MKRN1 proteins, the wild-type (1-482), point mutant (H307E) and deletion mutant (1-267) sequences were cloned into the pGEX-6P-1 (GE Healthcare Life Sciences) plasmid. The plasmid expressing Flag-E1B55K was generated by recloning the HAdV-C2 E1B55K cDNA from the pCMVE1B55K plasmid (60) into the pcDNA3.1-Flag plasmid. The plasmids expressing HAdV-C5 Flag-E4orf6 (61) and 6xHis-ubiquitin (62) were kindly provided by Drs. Paola Blanchette and Dimitris

355 Xirodimas, respectively. The plasmids encoding codon-optimized GST-pVII(wt), GST-
356 pVII(Δ24), pVII(wt)-Flag and pVII(Δ24)-Flag proteins have been described before (12).
357 The H1299, HEK293, A549 and U2OS cell lines were originally obtained from
358 the American Type Culture Collection (ATCC). All cell lines were grown in Dulbecco's
359 Modified Eagle Medium (DMEM, Invitrogen) supplemented with 10% fetal calf serum
360 (FCS, PAA) and penicillin-streptomycin (PEST) solution (Gibco) in a 7% CO_2
361 containing cell incubator. Stable HeLa cell line expressing codon-optimized pVII(wt)-
362 Flag was generated using the Flp-In™ recombination system in the HeLa-Flp-In T-Rex
363 cell line (63). All transfections were performed using Turbofect™ transfection reagent
364 (Thermo Scientific) according to the manufacturer's instructions.
365
366 **HAdV-C5 infections**
367 The following viruses were used: wild-type HAdV-C5 (generously provided by Prof.
368 Göran Akusjärvi) and E1B55K-deficient HAdV-C2 (dl1520) (54). Replication-competent
369 HAdV-C5 expressing the pVII-Flag fusion protein (HAdV-pVII-Flag) was generated
370 using pTG3602 as background viral DNA (64). The pTG3602 plasmid was co-
371 transformed with linearized donor DNA containing the HAdV-C5 pVII sequence fused
372 in-frame with the Flag-epitope tag sequence and chloramphenicol resistance gene into *E.*
373 *coli* BJ5183 cells (Agilent Technologies). Following the recombination, the positive
374 clones were selected with chloramphenicol and analyzed with PCR and sequencing. After
375 removal of the chloramphenicol resistance gene with SwaI restriction enzyme cleavage,
376 the plasmid was amplified and cleaved with PacI restriction enzyme to remove the
377 ampicillin resistance gene. Finally, the PacI linearized plasmid was transfected into

HEK293 cells using Turbofect™ reagent. The HAdV-pVII-Flag virus was amplified in 911 cells and purified by CsCl gradient centrifugation. Virus infections and titrations were done as described previously (65). The multiplicity of infection (FFU/cell; fluorescence forming units/per cell) is indicated in the respective figure legends.

Other virus infections

HCV: Huh7.5 cells were infected in 12-well plates for 48 h using the HCV genotype 2a strain clone pFK-JFH1/J6/C-846-dg (pFK-JC1) at MOI of 0.5. Cells were lysed in lysis buffer (0.5 % NP-40, 5M NaCl, 0.5 mM EDTA, 1M Tris-HCl [pH 7.5], 0,075g EGTA, 1% Triton X-100, 10% Glycerol, 10mM $Na_4P_2O_7$ in 50 ml) containing cOmplete protease inhibitors (Roche). HBV: HepaRG cells were cultured in Williams medium containing 10% FCS (ThermoFisher Scientific) and 1% PEST, 1% non-essential amino acids, 2mmol/L L-glutamine and 1% of sodium pyruvate (all from GIBCO), Insulin Rapid (Sanofi Aventis), Gentamycin (Ratiopharm), Hydrocortison (Pfizer Inc.,). For differentiation 1.8% of DMSO was added to the growth media. HepaRG cells were differentiated for a time period of four weeks. Infection was carried out using HBV at MOI of 200 for 24 h and washed the following day. Cells were lysed as indicated above 12 days post-infection. MV: Vero cells were plated in 12-well plates and infected with rMVrEdt-eGFP (kindly provided by Prof. Bert Rima, (66) and Prof. Jürgen Schneider-Schaulies) at MOI of 0.1. Cells were lysed 48 hpi as indicated above. VSV: Huh7.5 cells were plated in 12-well plates and infected with VSV*ΔG(LCMVgp) at MOI of 0.6 (kind gift of Prof. Dr. Gert Zimmer, (67)). Cells were lysed 18 hpi as indicated above. As both MVeGFP and VSV*ΔG(LCMVgp) express GFP, the infections were confirmed with

fluorescence monitoring using an inverted microscope CKX41 (Olympus) with an LCachN/10X/0.40 Phc/1/FN22 UIS objective (Fig. S4). HIV-1: LC5-RIC cells were infected with HIV-1 LAI Infectious Molecular Clone (pLAI.2) (68) and lysed 48 hpi as indicated above.

Antibodies and chemicals

The following primary antibodies were used: anti-mouse Flag (Sigma, M2, F1804), anti-rabbit Flag (Sigma, F7425), anti-rabbit HA (Santa Cruz, sc-805), anti-rabbit HMGB2 (Abcam, ab67282), anti-mouse C1QBP (Santa Cruz, sc-23885), anti-rabbit MKRN1 (Bethyl laboratories, A300-990A), anti-rabbit SET (Novus bio, NBP1-30888), anti-rabbit ACF1(BAZ1A) (Novus bio, NB100-61042), anti-rabbit CHD3 (Novus bio, NB100-60412), anti-mouse GAPDH (Ambion, Am4300), anti-mouse Mre11 (Abcam, ab214), anti-mouse His (Clontech, 631212), anti-mouse ubiquitin (FK2, Enzo BML-PW8810), anti-goat Actin (Santa Cruz, sc-1616), anti-rabbit GST (Santa Cruz, sc-33614), anti-mouse E1A (EMD Millipore, DP11-UG100), anti-mouse E1B55K (2A6, (69)), anti-rabbit GFP (Clontech, 632376), anti-HCV core, anti-mouse HIV-1 p24 (Chemicon international, MAB880-A), anti-rabbit Measles virus nucleoprotein NP (Covalab, pab0035) and anti-rabbit HAdV-5 Capsid (Abcam, ab6982). To inhibit proteasome, MG132 (Sigma, C2211, dissolved in DMSO) was used at a final concentration of 25 μM for 4 h unless otherwise specified in the figure legends. Control cells were treated only with DMSO. To inhibit protein synthesis, cells were treated with cycloheximide (Sigma, C4859, dissolved in DMSO) at a final concentration of 100 μg/ml.

424 **Yeast Two-Hybrid Analysis**

425 Yeast two-hybrid screening was performed by Hybrigenics Services, S.A.S., Paris,
426 France (http://www.hybrigenics-services.com). The codon-optimized coding sequence
427 for HAdV-C5 pVII (12) was PCR-amplified and cloned into the pB29 vector as an N-
428 terminal fusion to LexA (N-pVII-LexA-C). The generated construct was used as bait to
429 screen a random-primed Human Lung Cancer cDNA library constructed into the pP6
430 vector. 104 million clones (10-fold the complexity of the library) were screened using a
431 mating approach with YHGX13 (Y187 ade2-101::loxP-kanMX-loxP, matα) and
432 L40ΔGal4 (matα) yeast strains as previously described (70). 253 His+ colonies were
433 selected on a medium lacking tryptophan, leucine and histidine. The prey fragments of
434 the positive clones were amplified by PCR and sequenced at their 5' and 3' junctions to
435 identify the corresponding interacting proteins in the GenBank database (NCBI). A
436 confidence score (PBS, for Predicted Biological Score) was attributed to each interaction.
437 The PBS relies on two different levels of analysis. First, a local score takes into account
438 the redundancy and independence of prey fragments, as well as the distribution of reading
439 frames and stop codons in overlapping fragments. Second, a global score takes into
440 account the interactions found in all the screens performed at Hybrigenics using the same
441 library. This global score represents the probability of an interaction being nonspecific.
442 For practical use, the scores are divided into four categories, from A (highest confidence)
443 to D (lowest confidence).
444
445 ***In situ* Proximity Ligation Assay (PLA)**

446 Proximity ligation assay was carried out using reagents and instructions from Duolink II
447 kit (Olink Biosciences). Briefly, the HeLa-pVII(wt)-Flag cells were treated with
448 doxycycline (final concentration 0.2 μg/ml) to induce pVII(wt)-Flag protein expression
449 (71). Thirty-six hours post-induction the cells were washed twice with PBS, fixed with
450 3% paraformaldehyde for 15 min and permeabilized with 0.05% Triton in PBS for 15
451 min at room temperature. After blocking the cells with Duolink II blocking solution
452 overnight at 4°C, the slides were incubated with primary antibodies in a humidity
453 chamber for 1 h. Due to the antibody specificity requirement in the PLA assay, the anti-
454 mouse Flag antibody was combined with anti-rabbit antibodies (HMGB2, MKRN1, SET,
455 BAZ1A, CHD3). An exception was anti-mouse C1QBP antibody, which was combined
456 with anti-rabbit Flag antibody. The slides were washed 3 × 5 min with TBS-T (TBS +
457 0.05% Tween 20) prior to incubation with anti-mouse and anti-rabbit secondary probes
458 (Duolink II) for 90 min at 37°C. The ligation solution containing the Duolink ligase
459 (Duolink II) was applied to the TBS-T washed slides for 30 min at 37°C. Further, the
460 slides were washed with TBS-T and 40 μl of amplification solution was added to each
461 sample and incubated in a pre-heated humidity chamber for 90 min at 37°C. Thereafter,
462 the slides were washed once in TBS, stained with Hoechst dye and mounted with 10 μl
463 SlowFade mounting medium (Life Technologies). Labeled cells were visualized with a
464 Zeiss AxioPlan2 epi-microscope. Image analysis and signal quantification were
465 performed with the DuolinkImage Tool software (Olink Bioscience).
466
467 **Cell lysates and Western blot**
468 In general cells were lysed in RIPA buffer (12) for 20 min on ice, sonicated and

centrifuged at 15000 rpm, 4°C for 15 min. When the whole cell lysates were prepared from H1299 cells expressing the Flag-E1B55K and Flag-E4orf6 proteins (Fig. 4), the whole cell lysates were made as described in (61). Western blot membranes, either nitrocellulose or PVDF, were incubated with primary antibodies overnight at 4°C followed by incubation with the fluorescent-labeled secondary antibodies (IRDye®, LI-COR). The membranes were scanned using the Odyssey scanner (LI-COR) and the protein signals were quantified using Image Studio Software (LI-COR) (12).

Immunoprecipitation

Approximately 8×10^6 H1299 cells were either transfected or infected with HAdV-pVII-Flag virus. The cells were lysed in lysis buffer (150mM NaCl, 1mM EDTA, 0.5% NP-40, 0.5% Triton X-100, 0.1% sodium deoxycholate, 50mM Tris-HCl [pH 7.5], 1mM DTT and cOmplete protease inhibitors (Roche) for 30 min at 4°C. The soluble cell lysates were incubated with an anti-Flag (M2) coupled Sepharose beads (Sigma) for 2 h at 4°C. The beads were washed 3 × 1ml in lysis buffer, bound proteins were eluted with 2 × SDS-Loading dye and separated on SDS-PAGE.

GST pull-down assay

The GST pull-down assay was done as described previously (12). Approximately 2 µg of Glutathione Sepharose beads-bound GST and GST-pVII(wt or Δ24) proteins were incubated with H1299 whole cell lysates expressing the Flag-MKRN1(1-482), HA-MKRN1(1-482), HA-MKRN1(1-267), HA-MKRN1(112-267), HA-MKRN1(112-482) proteins at room temperature for 1 h. The beads were washed extensively with washing

buffer (25mM Hepes-KOH [pH 7.4], 12.5mM MgCl2, 200mM KCl, 0.1mM EDTA, 10% glycerol, 0.1% NP-40). The bound proteins were separated on 12% SDS-PAGE, followed by Western blot detection.

GST-MKRN1 purification

The BL21(DE3)-RIPL cells (Agilent Technologies) transformed with the pGEX-6P-MKRN1(wt), pGEX-6P-MKRN1(1-267) and pGEX-6P-MKRN1(H307E) were grown at 37°C in LB medium to OD_{600} 0.5-0.6. Protein expression was induced with 1mM IPTG for 4 h at 37°C. The cell pellets were lysed in lysis buffer (50mM Tris-HCl [pH 7.5], 150mM NaCl, 0.05% NP40, 1mM DTT, 0.25mg lysozyme and protease inhibitors). Cell lysates were sonicated, filtrated through 0,45 µm filter and purified using a GSTrap™ FF column (GE Healthcare) in ÄKTAxpress system (GE Healthcare) according to the manufacturer's recommendations. The column was equilibrated and washed in washing buffer (50mM Tris-HCl [pH 7.5], 150mM NaCl) and the proteins were eluted in washing buffer supplemented with 10 mM reduced glutathione (Sigma). Purified proteins were dialyzed against storage buffer (PBS+20% glycerol).

In vivo ubiquitination assay

The experiments were performed as described before (62). Briefly, H1299 cells were transfected with plasmids expressing the HA-MKRN1(wt), HA-MKRN1(1-267), HA-MKRN1(H307E), 6xHis-ubiquitin, pVII(wt)-Flag and pVII(Δ24)-Flag proteins. Thirty-six hours post-transfection the cells were treated with MG132 (10µM, 4h) followed by cell lysis in buffer containing 6M guanidine, 10mM β-mercaptoethanol, 5mM N-

ethylmaleimide and 5mM imidazole. The cell lysates were incubated with nickel-coupled agarose beads (Ni-NTA beads, Qiagen) by rotating at 4°C overnight. The beads were washed with buffer containing 8M urea, 10mM β-mercaptoethanol and 0.1% NP-40. Finally, the proteins were eluted from the Ni-NTA beads with a sample buffer containing 0.72M β-mercaptoethanol and 200mM imidazole.

In vitro ubiquitination assay

Equal amounts of the purified GST-MKRN1 (wt, H307E, 1-267) were mixed with purified His-UbE1, His-UbcH5a, Ubiquitin-MAX™ proteins (all from Viva Biosciences) in a reaction buffer containing 40mM Tris-HCl [pH 7.5], 1mM DTT, 5mM $MgCl_2$, 2mM ATP according to the manufacturer's recommendations. After incubation at 37°C for 2 h, reactions were terminated with 2 × SDS-Loading dye.

RNA extraction and qRT-PCR

Total RNA extraction, cDNA synthesis with random primers and qRT-PCR reactions were performed as previously described (65). The following MKRN1 primers were used: tp575 (5'-GCAGCAAGGGATGACTTTGT-3) and tp576 (5'-TGTATTTATGGAGACCGCTGC-3). Relative MKRN1 mRNA expression was calculated after normalization to the HPRT1 mRNA levels using $2^{-\Delta\Delta CT}$ method (72).

ACKNOWLEDGMENTS

This work was supported by Gösta Näslund Minnesfond (RI), Marcus Borgströms Foundation (TP), Åke Wibergs Foundation (M14-0155, TP), the Swedish Cancer Society

538 (CAN 2013/350, TP) and the Swedish Research Council through a grant to the Uppsala
539 RNA Research Centre (2006-5038-36531-16, TP). KM is supported by Erasmus Mundus
540 LOTUS+ program. SS is supported by the Else Kröner-Fresenius-Stiftung, the Deutsche
541 Forschungsgemeinschaft DFG (SFB TRR179), Deutsche Krebshilfe e.V. and the Dräger
542 Stiftung e. V. *In situ* PLA was performed by the PLA Proteomics facility, which is
543 supported by Science for Life Laboratory. We would also like to thank Drs. Anna Rostedt
544 Punga, Arnold Berk, Agata Zieba, Stephen Taylor, Paola Blanchette, Anders Sundqvist,
545 Melissa Navarro, Dimitris Xirodimas, Göran Akusjärvi, Bert Rima, Gert Zimmer, Ruth
546 Brack-Werner, Alexander Herrmann, Sawinee Masser, Jürgen Schneider-Schaulies for
547 kindly providing the reagents, Dr. Mårten Larsson for protein purification, Dr. Daniel
548 Öberg for generously designing the HAdV-pVII-Flag virus cloning strategy, and Dr.
549 Marta Lewandowska for proofreading the manuscript.

550

551 **REFERENCES**

552 1. **Lion T.** 2014. Adenovirus infections in immunocompetent and
553 immunocompromised patients. Clin Microbiol Rev **27:**441-462.
554 2. **Assadian F, Sandstrom K, Bondeson K, Laurell G, Lidian A, Svensson C,**
555 **Akusjarvi G, Bergqvist A, Punga T.** 2016. Distribution and Molecular
556 Characterization of Human Adenovirus and Epstein-Barr Virus Infections in
557 Tonsillar Lymphocytes Isolated from Patients Diagnosed with Tonsillar Diseases.
558 PLoS One **11:**e0154814.
559 3. **Russell WC.** 2009. Adenoviruses: update on structure and function. The Journal
560 of general virology **90:**1-20.

4. **Alestrom P, Akusjarvi G, Lager M, Yeh-kai L, Pettersson U.** 1984. Genes encoding the core proteins of adenovirus type 2. The Journal of biological chemistry **259:**13980-13985.

5. **Benevento M, Di Palma S, Snijder J, Moyer CL, Reddy VS, Nemerow GR, Heck AJ.** 2014. Adenovirus composition, proteolysis, and disassembly studied by in-depth qualitative and quantitative proteomics. J Biol Chem **289:**11421-11430.

6. **Blainey PC, Graziano V, Perez-Berna AJ, McGrath WJ, Flint SJ, San Martin C, Xie XS, Mangel WF.** 2013. Regulation of a viral proteinase by a peptide and DNA in one-dimensional space: IV. viral proteinase slides along DNA to locate and process its substrates. J Biol Chem **288:**2092-2102.

7. **Ruzindana-Umunyana A, Imbeault L, Weber JM.** 2002. Substrate specificity of adenovirus protease. Virus Res **89:**41-52.

8. **Sung MT, Cao TM, Lischwe MA, Coleman RT.** 1983. Molecular processing of adenovirus proteins. J Biol Chem **258:**8266-8272.

9. **Webster A, Russell S, Talbot P, Russell WC, Kemp GD.** 1989. Characterization of the adenovirus proteinase: substrate specificity. The Journal of general virology **70 (Pt 12):**3225-3234.

10. **Ortega-Esteban A, Condezo GN, Perez-Berna AJ, Chillon M, Flint SJ, Reguera D, San Martin C, de Pablo PJ.** 2015. Mechanics of Viral Chromatin Reveals the Pressurization of Human Adenovirus. ACS Nano **9:**10826-10833.

11. **Perez-Berna AJ, Marion S, Chichon FJ, Fernandez JJ, Winkler DC, Carrascosa JL, Steven AC, Siber A, San Martin C.** 2015. Distribution of

583 DNA-condensing protein complexes in the adenovirus core. Nucleic Acids Res
584 **43:**4274-4283.
585 12. **Inturi R, Thaduri S, Punga T.** 2013. Adenovirus precursor pVII protein stability
586 is regulated by its propeptide sequence. PLoS One **8:**e80617.
587 13. **Chatterjee PK, Vayda ME, Flint SJ.** 1986. Adenoviral protein VII packages
588 intracellular viral DNA throughout the early phase of infection. The EMBO
589 journal **5:**1633-1644.
590 14. **Lischwe MA, Sung MT.** 1977. A histone-like protein from adenovirus
591 chromatin. Nature **267:**552-554.
592 15. **Vayda ME, Rogers AE, Flint SJ.** 1983. The structure of nucleoprotein cores
593 released from adenovirions. Nucleic acids research **11:**441-460.
594 16. **Corden J, Engelking HM, Pearson GD.** 1976. Chromatin-like organization of
595 the adenovirus chromosome. Proc Natl Acad Sci U S A **73:**401-404.
596 17. **Ostapchuk P, Suomalainen M, Zheng Y, Boucke K, Greber UF, Hearing P.**
597 2017. The adenovirus major core protein VII is dispensable for virion assembly
598 but is essential for lytic infection. PLoS Pathog **13:**e1006455.
599 18. **Komatsu T, Dacheux D, Kreppel F, Nagata K, Wodrich H.** 2015. A Method
600 for Visualization of Incoming Adenovirus Chromatin Complexes in Fixed and
601 Living Cells. PLoS One **10:**e0137102.
602 19. **Wodrich H, Cassany A, D'Angelo MA, Guan T, Nemerow G, Gerace L.** 2006.
603 Adenovirus core protein pVII is translocated into the nucleus by multiple import
604 receptor pathways. Journal of virology **80:**9608-9618.

20. **Cassany A, Ragues J, Guan T, Begu D, Wodrich H, Kann M, Nemerow GR, Gerace L.** 2015. Nuclear import of adenovirus DNA involves direct interaction of hexon with an N-terminal domain of the nucleoporin Nup214. J Virol **89:**1719-1730.

21. **Karen KA, Hearing P.** 2011. Adenovirus core protein VII protects the viral genome from a DNA damage response at early times after infection. Journal of virology **85:**4135-4142.

22. **Komatsu T, Haruki H, Nagata K.** 2011. Cellular and viral chromatin proteins are positive factors in the regulation of adenovirus gene expression. Nucleic acids research **39:**889-901.

23. **Komatsu T, Nagata K.** 2012. Replication-uncoupled histone deposition during adenovirus DNA replication. Journal of virology **86:**6701-6711.

24. **Haruki H, Okuwaki M, Miyagishi M, Taira K, Nagata K.** 2006. Involvement of template-activating factor I/SET in transcription of adenovirus early genes as a positive-acting factor. Journal of virology **80:**794-801.

25. **Matsumoto K, Okuwaki M, Kawase H, Handa H, Hanaoka F, Nagata K.** 1995. Stimulation of DNA transcription by the replication factor from the adenovirus genome in a chromatin-like structure. The Journal of biological chemistry **270:**9645-9650.

26. **Okuwaki M, Nagata K.** 1998. Template activating factor-I remodels the chromatin structure and stimulates transcription from the chromatin template. The Journal of biological chemistry **273:**34511-34518.

27. **Johnson JS, Osheim YN, Xue Y, Emanuel MR, Lewis PW, Bankovich A, Beyer AL, Engel DA.** 2004. Adenovirus protein VII condenses DNA, represses transcription, and associates with transcriptional activator E1A. Journal of virology **78:**6459-6468.

28. **Avgousti DC, Herrmann C, Kulej K, Pancholi NJ, Sekulic N, Petrescu J, Molden RC, Blumenthal D, Paris AJ, Reyes ED, Ostapchuk P, Hearing P, Seeholzer SH, Worthen GS, Black BE, Garcia BA, Weitzman MD.** 2016. A core viral protein binds host nucleosomes to sequester immune danger signals. Nature **535:**173-177.

29. **Avgousti DC, Della Fera AN, Otter CJ, Herrmann C, Pancholi NJ, Weitzman MD.** 2017. Adenovirus core protein VII down-regulates the DNA damage response on the host genome. J Virol doi:10.1128/JVI.01089-17.

30. **Chondrogianni N, Gonos ES.** 2012. Structure and function of the ubiquitin-proteasome system: modulation of components. Prog Mol Biol Transl Sci **109:**41-74.

31. **Blanchette P, Branton PE.** 2009. Manipulation of the ubiquitin-proteasome pathway by small DNA tumor viruses. Virology **384:**317-323.

32. **Schreiner S, Wimmer P, Dobner T.** 2012. Adenovirus degradation of cellular proteins. Future Microbiol **7:**211-225.

33. **Wimmer P, Schreiner S.** 2015. Viral Mimicry to Usurp Ubiquitin and SUMO Host Pathways. Viruses **7:**4854-4872.

34. **Baker A, Rohleder KJ, Hanakahi LA, Ketner G.** 2007. Adenovirus E4 34k and E1b 55k oncoproteins target host DNA ligase IV for proteasomal degradation. J Virol **81:**7034-7040.

35. **Dallaire F, Blanchette P, Groitl P, Dobner T, Branton PE.** 2009. Identification of integrin alpha3 as a new substrate of the adenovirus E4orf6/E1B 55-kilodalton E3 ubiquitin ligase complex. Journal of virology **83:**5329-5338.

36. **Gupta A, Jha S, Engel DA, Ornelles DA, Dutta A.** 2013. Tip60 degradation by adenovirus relieves transcriptional repression of viral transcriptional activator EIA. Oncogene **32:**5017-5025.

37. **Querido E, Blanchette P, Yan Q, Kamura T, Morrison M, Boivin D, Kaelin WG, Conaway RC, Conaway JW, Branton PE.** 2001. Degradation of p53 by adenovirus E4orf6 and E1B55K proteins occurs via a novel mechanism involving a Cullin-containing complex. Genes & development **15:**3104-3117.

38. **Schreiner S, Burck C, Glass M, Groitl P, Wimmer P, Kinkley S, Mund A, Everett RD, Dobner T.** 2013. Control of human adenovirus type 5 gene expression by cellular Daxx/ATRX chromatin-associated complexes. Nucleic acids research **41:**3532-3550.

39. **Schreiner S, Kinkley S, Burck C, Mund A, Wimmer P, Schubert T, Groitl P, Will H, Dobner T.** 2013. SPOC1-mediated antiviral host cell response is antagonized early in human adenovirus type 5 infection. PLoS Pathog **9:**e1003775.

40. **Stracker TH, Carson CT, Weitzman MD.** 2002. Adenovirus oncoproteins inactivate the Mre11-Rad50-NBS1 DNA repair complex. Nature **418:**348-352.

671 41. **Gray TA, Hernandez L, Carey AH, Schaldach MA, Smithwick MJ, Rus K,**
672 **Marshall Graves JA, Stewart CL, Nicholls RD.** 2000. The ancient source of a
673 distinct gene family encoding proteins featuring RING and C(3)H zinc-finger
674 motifs with abundant expression in developing brain and nervous system.
675 Genomics **66:**76-86.
676 42. **Kim JH, Park SM, Kang MR, Oh SY, Lee TH, Muller MT, Chung IK.** 2005.
677 Ubiquitin ligase MKRN1 modulates telomere length homeostasis through a
678 proteolysis of hTERT. Genes Dev **19:**776-781.
679 43. **Kim JH, Park KW, Lee EW, Jang WS, Seo J, Shin S, Hwang KA, Song J.**
680 2014. Suppression of PPARgamma through MKRN1-mediated ubiquitination and
681 degradation prevents adipocyte differentiation. Cell Death Differ **21:**594-603.
682 44. **Ko A, Shin JY, Seo J, Lee KD, Lee EW, Lee MS, Lee HW, Choi IJ, Jeong JS,**
683 **Chun KH, Song J.** 2012. Acceleration of gastric tumorigenesis through MKRN1-
684 mediated posttranslational regulation of p14ARF. J Natl Cancer Inst **104:**1660-
685 1672.
686 45. **Lee EW, Kim JH, Ahn YH, Seo J, Ko A, Jeong M, Kim SJ, Ro JY, Park KM,**
687 **Lee HW, Park EJ, Chun KH, Song J.** 2012. Ubiquitination and degradation of
688 the FADD adaptor protein regulate death receptor-mediated apoptosis and
689 necroptosis. Nat Commun **3:**978.
690 46. **Lee EW, Lee MS, Camus S, Ghim J, Yang MR, Oh W, Ha NC, Lane DP,**
691 **Song J.** 2009. Differential regulation of p53 and p21 by MKRN1 E3 ligase
692 controls cell cycle arrest and apoptosis. EMBO J **28:**2100-2113.

693 47. **Lee MS, Jeong MH, Lee HW, Han HJ, Ko A, Hewitt SM, Kim JH, Chun KH,**
694 **Chung JY, Lee C, Cho H, Song J.** 2015. PI3K/AKT activation induces PTEN
695 ubiquitination and destabilization accelerating tumourigenesis. Nat Commun
696 **6:**7769.
697 48. **Ko A, Lee EW, Yeh JY, Yang MR, Oh W, Moon JS, Song J.** 2010. MKRN1
698 induces degradation of West Nile virus capsid protein by functioning as an E3
699 ligase. J Virol **84:**426-436.
700 49. **Finsterbusch T, Steinfeldt T, Doberstein K, Rodner C, Mankertz A.** 2009.
701 Interaction of the replication proteins and the capsid protein of porcine circovirus
702 type 1 and 2 with host proteins. Virology **386:**122-131.
703 50. **Cassar PA, Carpenedo RL, Samavarchi-Tehrani P, Olsen JB, Park CJ,**
704 **Chang WY, Chen Z, Choey C, Delaney S, Guo H, Guo H, Tanner RM,**
705 **Perkins TJ, Tenenbaum SA, Emili A, Wrana JL, Gibbings D, Stanford WL.**
706 2015. Integrative genomics positions MKRN1 as a novel ribonucleoprotein within
707 the embryonic stem cell gene regulatory network. EMBO Rep **16:**1334-1357.
708 51. **Omwancha J, Zhou XF, Chen SY, Baslan T, Fisher CJ, Zheng Z, Cai C,**
709 **Shemshedini L.** 2006. Makorin RING finger protein 1 (MKRN1) has negative
710 and positive effects on RNA polymerase II-dependent transcription. Endocrine
711 **29:**363-373.
712 52. **Haruki H, Gyurcsik B, Okuwaki M, Nagata K.** 2003. Ternary complex
713 formation between DNA-adenovirus core protein VII and TAF-Ibeta/SET, an
714 acidic molecular chaperone. FEBS Lett **555:**521-527.

53. **Xue Y, Johnson JS, Ornelles DA, Lieberman J, Engel DA.** 2005. Adenovirus protein VII functions throughout early phase and interacts with cellular proteins SET and pp32. Journal of virology **79:**2474-2483.

54. **Barker DD, Berk AJ.** 1987. Adenovirus proteins from both E1B reading frames are required for transformation of rodent cells by viral infection and DNA transfection. Virology **156:**107-121.

55. **Miroci H, Schob C, Kindler S, Olschlager-Schutt J, Fehr S, Jungenitz T, Schwarzacher SW, Bagni C, Mohr E.** 2012. Makorin ring zinc finger protein 1 (MKRN1), a novel poly(A)-binding protein-interacting protein, stimulates translation in nerve cells. J Biol Chem **287:**1322-1334.

56. **Torchy MP, Hamiche A, Klaholz BP.** 2015. Structure and function insights into the NuRD chromatin remodeling complex. Cellular and Molecular Life Sciences **72:**2491-2507.

57. **Lans H, Marteijn JA, Vermeulen W.** 2012. ATP-dependent chromatin remodeling in the DNA-damage response. Epigenetics Chromatin **5:**4.

58. **Bergstrom Lind S, Artemenko KA, Elfineh L, Zhao Y, Bergquist J, Pettersson U.** 2012. The phosphoproteome of the adenovirus type 2 virion. Virology **433:**253-261.

59. **Liu L, Oliveira NM, Cheney KM, Pade C, Dreja H, Bergin AM, Borgdorff V, Beach DH, Bishop CL, Dittmar MT, McKnight A.** 2011. A whole genome screen for HIV restriction factors. Retrovirology **8:**94.

736 60. **Punga T, Akusjarvi G.** 2003. Adenovirus 2 E1B-55K protein relieves p53-
737 mediated transcriptional repression of the survivin and MAP4 promoters. FEBS
738 Lett **552:**214-218.
739 61. **Cheng CY, Gilson T, Dallaire F, Ketner G, Branton PE, Blanchette P.** 2011.
740 The E4orf6/E1B55K E3 ubiquitin ligase complexes of human adenoviruses
741 exhibit heterogeneity in composition and substrate specificity. J Virol **85:**765-
742 775.
743 62. **Xirodimas D, Saville MK, Edling C, Lane DP, Lain S.** 2001. Different effects
744 of p14ARF on the levels of ubiquitinated p53 and Mdm2 in vivo. Oncogene
745 **20:**4972-4983.
746 63. **Hewitt L, Tighe A, Santaguida S, White AM, Jones CD, Musacchio A, Green**
747 **S, Taylor SS.** 2010. Sustained Mps1 activity is required in mitosis to recruit O-
748 Mad2 to the Mad1-C-Mad2 core complex. The Journal of cell biology **190:**25-34.
749 64. **Chartier C, Degryse E, Gantzer M, Dieterle A, Pavirani A, Mehtali M.** 1996.
750 Efficient generation of recombinant adenovirus vectors by homologous
751 recombination in Escherichia coli. J Virol **70:**4805-4810.
752 65. **Inturi R, Kamel W, Akusjarvi G, Punga T.** 2015. Complementation of the
753 human adenovirus type 5 VA RNAI defect by the Vaccinia virus E3L protein and
754 serotype-specific VA RNAIs. Virology **485:**25-35.
755 66. **Duprex WP, McQuaid S, Roscic-Mrkic B, Cattaneo R, McCallister C, Rima**
756 **BK.** 2000. In vitro and in vivo infection of neural cells by a recombinant measles
757 virus expressing enhanced green fluorescent protein. J Virol **74:**7972-7979.

67. **Berger Rentsch M, Zimmer G.** 2011. A vesicular stomatitis virus replicon-based bioassay for the rapid and sensitive determination of multi-species type I interferon. PLoS One **6:**e25858.

68. **Kremb S, Helfer M, Heller W, Hoffmann D, Wolff H, Kleinschmidt A, Cepok S, Hemmer B, Durner J, Brack-Werner R.** 2010. EASY-HIT: HIV full-replication technology for broad discovery of multiple classes of HIV inhibitors. Antimicrob Agents Chemother **54:**5257-5268.

69. **Sarnow P, Sullivan CA, Levine AJ.** 1982. A monoclonal antibody detecting the adenovirus type 5-E1b-58Kd tumor antigen: characterization of the E1b-58Kd tumor antigen in adenovirus-infected and -transformed cells. Virology **120:**510-517.

70. **Fromont-Racine M, Rain JC, Legrain P.** 1997. Toward a functional analysis of the yeast genome through exhaustive two-hybrid screens. Nat Genet **16:**277-282.

71. **Krzywkowski T, Ciftci S, Assadian F, Nilsson M, Punga T.** 2017. Simultaneous Single-Cell In Situ Analysis of Human Adenovirus Type 5 DNA and mRNA Expression Patterns in Lytic and Persistent Infection. J Virol **91**.

72. **Schmittgen TD, Livak KJ.** 2008. Analyzing real-time PCR data by the comparative C(T) method. Nat Protoc **3:**1101-1108.

FIGURE LEGENDS

Fig. 1. Proximal association of the precursor pVII(wt)-Flag protein and its interacting proteins. Proximity ligation assay (PLA) was performed in HeLa stable cell

line expressing the pVII(wt)-Flag protein after doxycycline treatment. The proteins analyzed for pVII(wt)-Flag binding are shown above the images. In the control reaction an irrelevant antibody (anti-HA) was used. Proximity ligation signals were amplified with rolling circle amplification (RCA) and are shown in red, whereas blue is Hoechst dye staining the nuclei. Quantification of the proximity ligation event is shown as RCA signals/per cell analyzed in triplicates. Bars denote the mean ± SD RCA signals/per cell. Unpaired t-test indicated significantly (**** $p<0.0001$, *** $p<0.001$, ** $p<0.01$, * $p<0.05$) higher numbers of RCA signals/cell in specific antibody samples compared to the control (anti-HA) sample.

Fig. 2. The precursor pVII protein interacts with MKRN1 in vitro and in vivo. A) H1299 cells were infected with HAdV-pVII-Flag virus (5 FFU/cell) for 20 h followed by immunoprecipitation with an anti-Flag antibody (lanes 2 and 5). Cells were treated with MG132 (4h, 25µM) at 16 hpi and collected at the same time as the non-MG132 treated cells (lanes 3 and 6). Detection of the HAdV-C5 E1A and cellular HMGB2 proteins was used as the specificity control. The arrowhead points to migration of the MKRN1 protein, whereas the asterisk indicates migration of the pVII-Flag protein. Western blot (WB). B) H1299 cell lysates transiently expressing the HA-MKRN1(wt) and pVII(wt)-Flag or pVII(Δ24)-Flag proteins were immunoprecipitated with an anti-Flag antibody. Relative binding of HA-MKRN1 from two independent experiments is shown below the image after normalization to the input values. The asterisk indicates migration of the Flag antibody light chain. Note that HA-MKRN1 has some unspecific binding to Flag-coupled beads (lane 4). C) GST-pVII(wt and Δ24) pull-down with H1299 whole cell lysates

804 expressing the Flag-MKRN1(wt) protein. The arrowhead indicates migration of full-
805 length GST-pVII proteins, whereas the asterisk marks migration of the GST protein. D)
806 Illustration of the MKRN1 mutant proteins. Labeling of zinc finger motifs (ZnF) and
807 RING finger (RING) domain is based on Uniprot (www.uniprot.org) annotation. E) GST-
808 pVII(wt) pull-down experiment with H1299 whole cell lysates expressing the indicated
809 HA-MKRN1 proteins. Quantitative binding of the respective HA-MKRN1 proteins to
810 GST-pVII(wt) is shown after normalization to input values (% of input). Arrowhead
811 indicates migration of the GST-pVII(wt) protein.
812
813 **Fig. 3. The MKRN1 protein undergoes proteasomal degradation in HAdV-C5-**
814 **infected cells.** A) H1299 cells were infected with HAdV-C5 (10 FFU/cell). Whole cell
815 lysates were collected at indicated hours post infection (hpi) and analyzed by WB. The
816 arrowhead indicates migration of MKRN1, whereas the asterisk (*) marks an unspecific
817 protein occasionally detected with MKRN1 antibody. B) HAdV-C5-infected (10
818 FFU/cell) H1299 cells were treated at 20 hpi with MG132 (4h, 25μM). All cell samples
819 were harvested 24 hpi and analyzed by WB. Detection of the HAdV-C5 E1A protein acts
820 as a positive control for MG132 treatment. C) H1299 cells were infected with HAdV-C5
821 (10 FFU/cell) for the indicated time points. Relative MKRN1 mRNA expression was
822 analyzed by qRT-PCR after normalization to HPRT1 mRNA. Bars denote the mean ± SD
823 MKRN1 expression. D) H1299 cells were infected with HAdV-pVII-Flag virus (10
824 FFU/cell) and harvested at the indicated hpi. Expression of the HAdV-encoded pVII-Flag
825 was detected with an anti-Flag antibody. E) A549, U2OS and HEK293 cells were

826 infected with HAdV-C5 (10 FFU/cell), harvested at the indicated hpi and analyzed for
827 protein expression as in panel A and D.
828
829 **Fig. 4. The MKRN1 protein is degraded independently of the E1B55K and E4orf6**
830 **proteins.** A) H1299 cells were transiently transfected with plasmids expressing the Flag-
831 E1B55K and/or Flag-E4orf6 proteins. Whole cell extracts were made at the indicated
832 hours post-transfection (hpt) and proteins were detected by WB. Detection of the Mre11
833 protein was used to confirm the functionality of the E1B55K/E4orf6 complex. Relative
834 quantification of the Mre11 and MKRN1 proteins in Flag-E1B55K and Flag-E4orf6
835 expressing cells (lanes 4 and 8) compared to control transfected cells (lanes 1 and 5) is
836 shown on the graph below the WB images. The Mre11 and MKRN1 protein levels were
837 normalized to GAPDH protein. B) H1299 cells were infected (10 FFU/cell) with HAdV-
838 C5 (wt) and HAdV-C2 (dl1520) viruses. Whole cell lysates were analyzed by WB at 24
839 hpi and 48 hpi. * denotes unspecific protein recognized with the anti-capsid antibody
840 after WB membrane stripping.
841
842 **Fig. 5. The precursor pVII protein enhances MKRN1 self-ubiquitination.** A)
843 pVII(wt)-Flag enhances MKRN1 ubiquitination *in vivo*. H1299 cells were transfected
844 with plasmids expressing the 6xHis-ubiquitin, HA-MKRN1 (wt or 1-267), pVII-Flag (wt
845 or Δ24) proteins. Cells were treated 36 hpt with MG132 (10 μM, 4h). Ubiquitinated
846 proteins were isolated using the nickel pull-down (Ni-NTA) approach and analyzed along
847 with the whole cell lysate input samples by WB. B) MKRN1(H307E) is resistant to
848 pVII(wt) enhanced ubiquitination. Ni-NTA pull-down in H1299 cells expressing HA-

MKRN1(wt or H307E), pVII(wt)-Flag and 6xHis-ubiquitin proteins. Cells were harvested and treated as described for panel A. Ubiquitin signals were quantitated and the relative level of HA-MKRN1 coupled His-ubiquitin (Ub-MKRN1) is shown below the first panel ("Ni-NTA pull-down WB:HA"). C) The pVII(wt)-Flag protein co-immunoprecipitates with HA-MKRN1 (wt, H307E, 1-267) in transiently transfected H1299 cells. The asterisk indicates detection of unspecific protein with an anti-HA antibody. D) MKRN1(H307E) is deficient in self-ubiquitination. *In vitro* ubiquitination assay was performed with the indicated recombinant His- and GST-tagged proteins in the presence of purified ubiquitin protein. Ubiquitinated GST-MKRN1 (Ub-MKRN1) was detected with an anti-ubiquitin (FK2) antibody. E) MKRN1(H307E) degradation is decelerated in virus-infected cells. H1299 cells were transiently transfected with plasmids expressing the HA-MKRN1(wt) or HA-MKRN1(H307E) proteins followed by HAdV-pVII-Flag infection (2 FFU/cell). Cells were treated at 48 hpi with cycloheximide and the whole cell lysates were prepared from cells harvested at 90, 180, 285 and 390 min post-treatment. The HA-tagged MKRN1 and actin proteins were quantified on WB and the relative HA-MKRN1 protein levels were calculated after normalization to actin. Mean ±SEM from two independent experiments is shown.

Fig. 6. The MKRN1 protein accumulation is downregulated in VSV and MV infected cells

Total protein lysates of cells either infected (+) or non-infected (-) with the indicated viruses were analyzed by WB. The arrowhead indicates migration of the endogenous MKRN1 protein. Relative accumulation of the MKRN1 protein is shown after

normalization to actin (MKRN1/Actin). Virus infections were confirmed with the following antibodies: anti-p24 (HIV-1), anti-core (HCV), anti-nucleoprotein NP (MV), anti-GFP (VSV) and anti-core (HBV). HCV, MV and VSV infections were confirmed on the same WB membrane as the MKRN1 and actin proteins, whereas HIV-1 and HBV infections were confirmed on a separate WB membrane.

Journal of Virology JVI Journal of Virology

879 TABLE 1 Identified precursor pVII interacting proteins in yeast two-hybrid screen

Official gene symbol	Official full name	Gene ID	Number of clones	PBS[a]
C1QBP	complement C1q binding protein	708	100	A
SET	SET nuclear proto-oncogene	6418	36	A
HMGB2	high mobility group box 2	3148	30	A
HMGB3	high mobility group box 3	3149	13	A
SETSIP	SET-like protein	646817	15	B
ZNF622	zinc finger protein 622	90441	4	C
CHD3	chromodomain helicase DNA binding protein 3	1107	4	D
MKRN1	makorin ring finger protein 1	23608	2	D
BAZ1A	bromodomain adjacent to zinc finger domain 1A	11177	1	D
CTPS1	CTP synthase 1	1503	1	D
RACK1	Receptor for activated C kinase 1	10399	1	D
PTGES3L-AARSD1	PTGES3L-AARSD1 readthrough	100885850	1	D
ARMCX2	armadillo repeat containing, X-linked 2	9823	1	D

880 [a]PBS= Predicted Biological Score

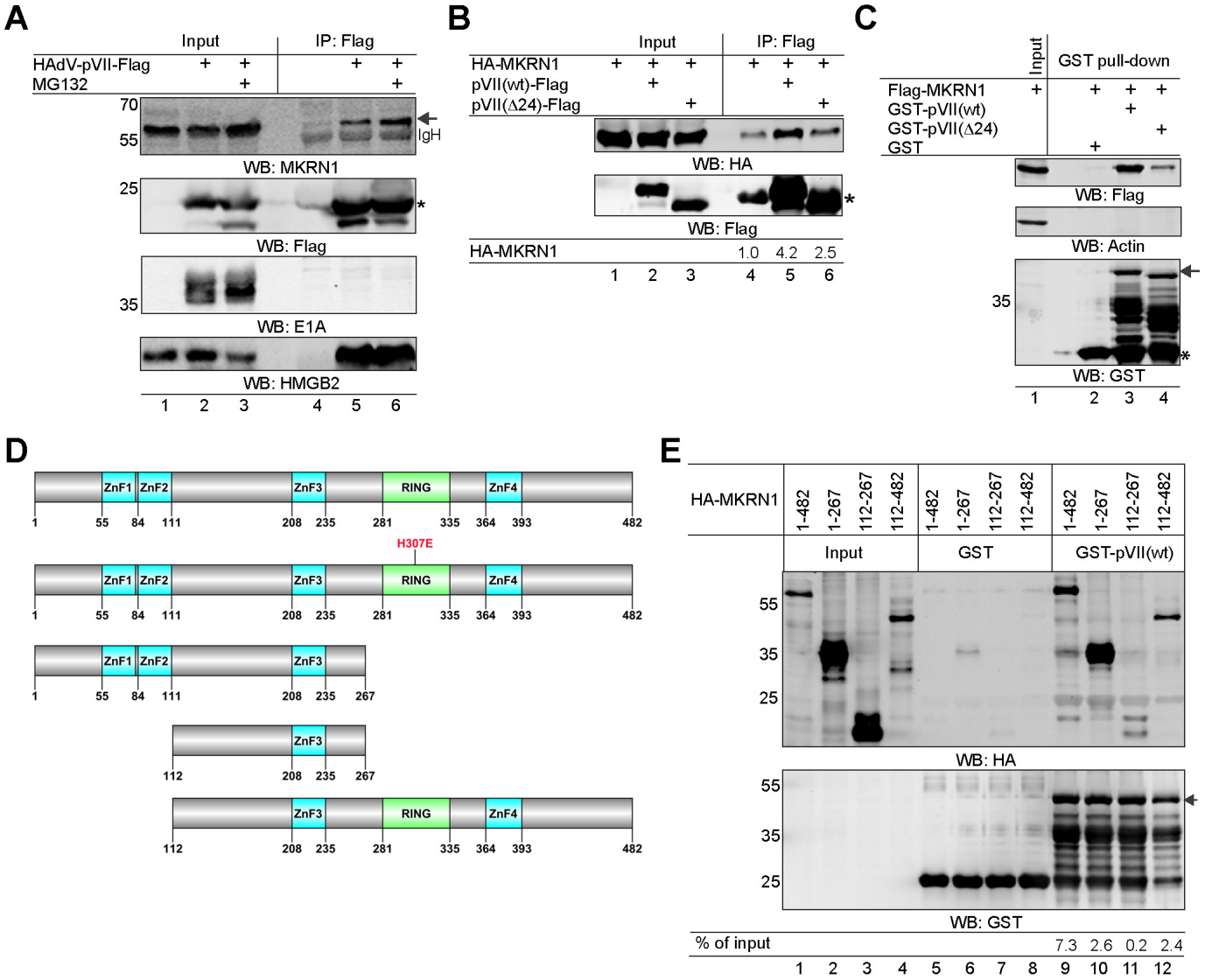

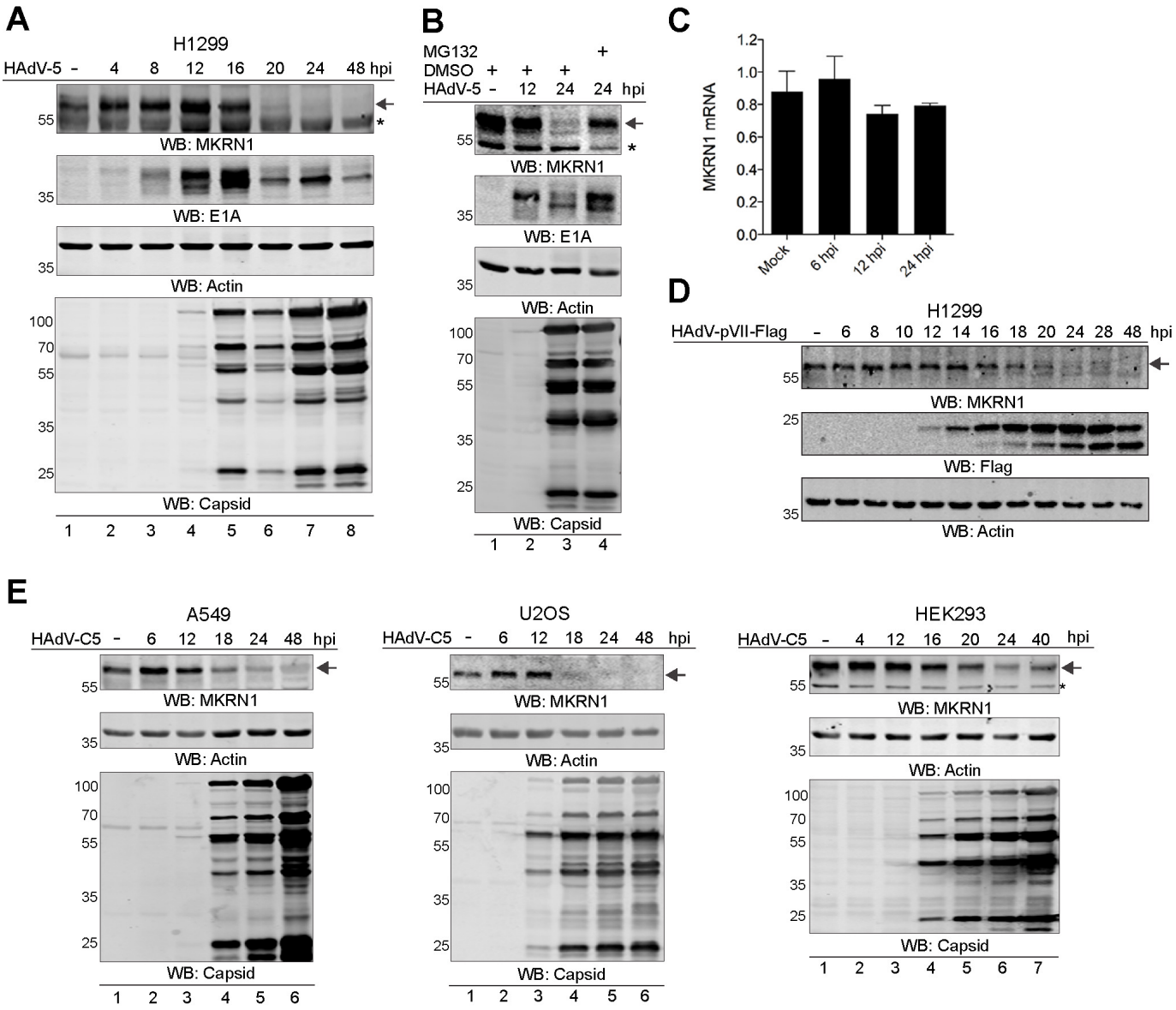

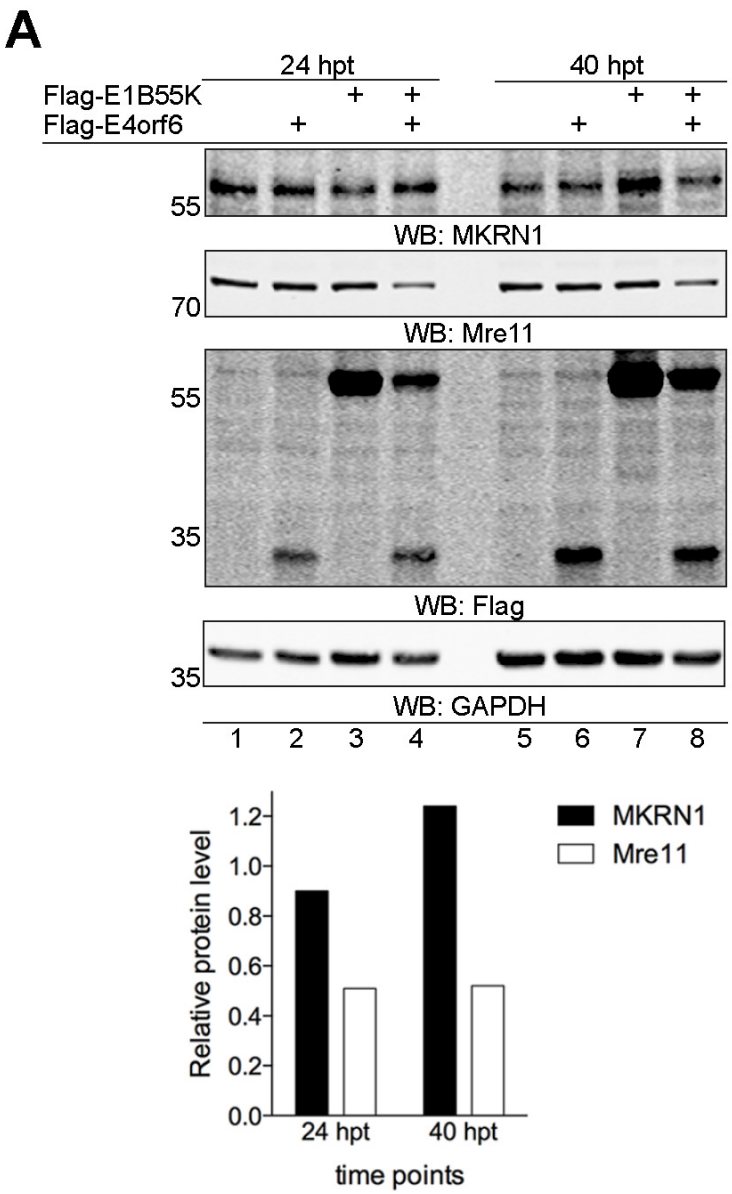

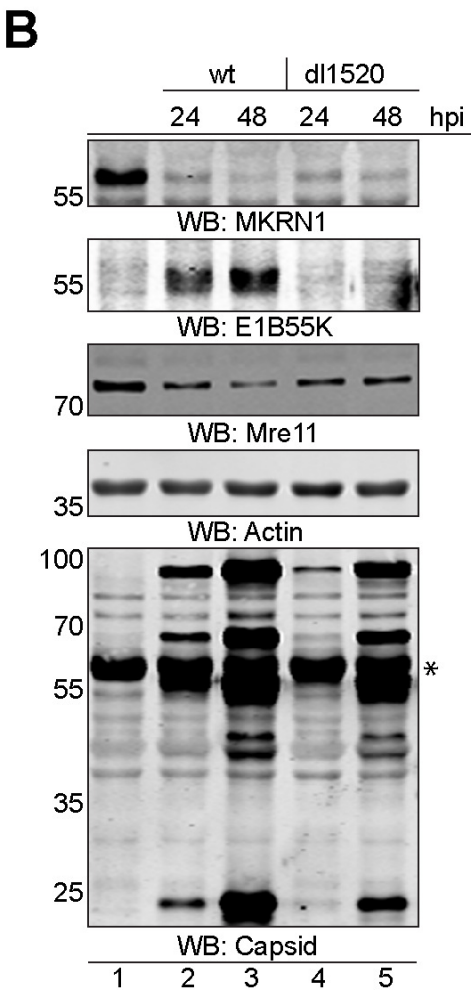

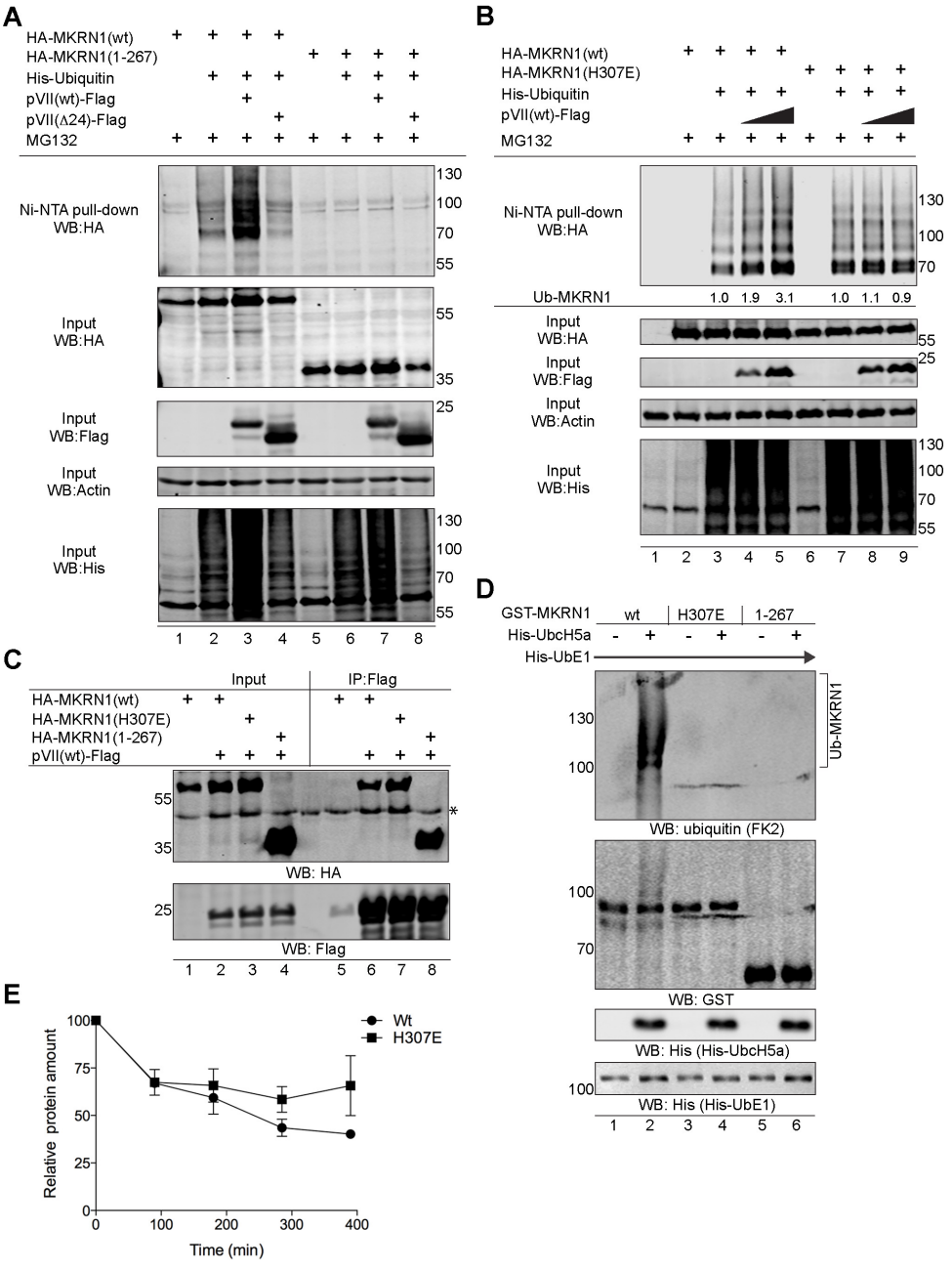

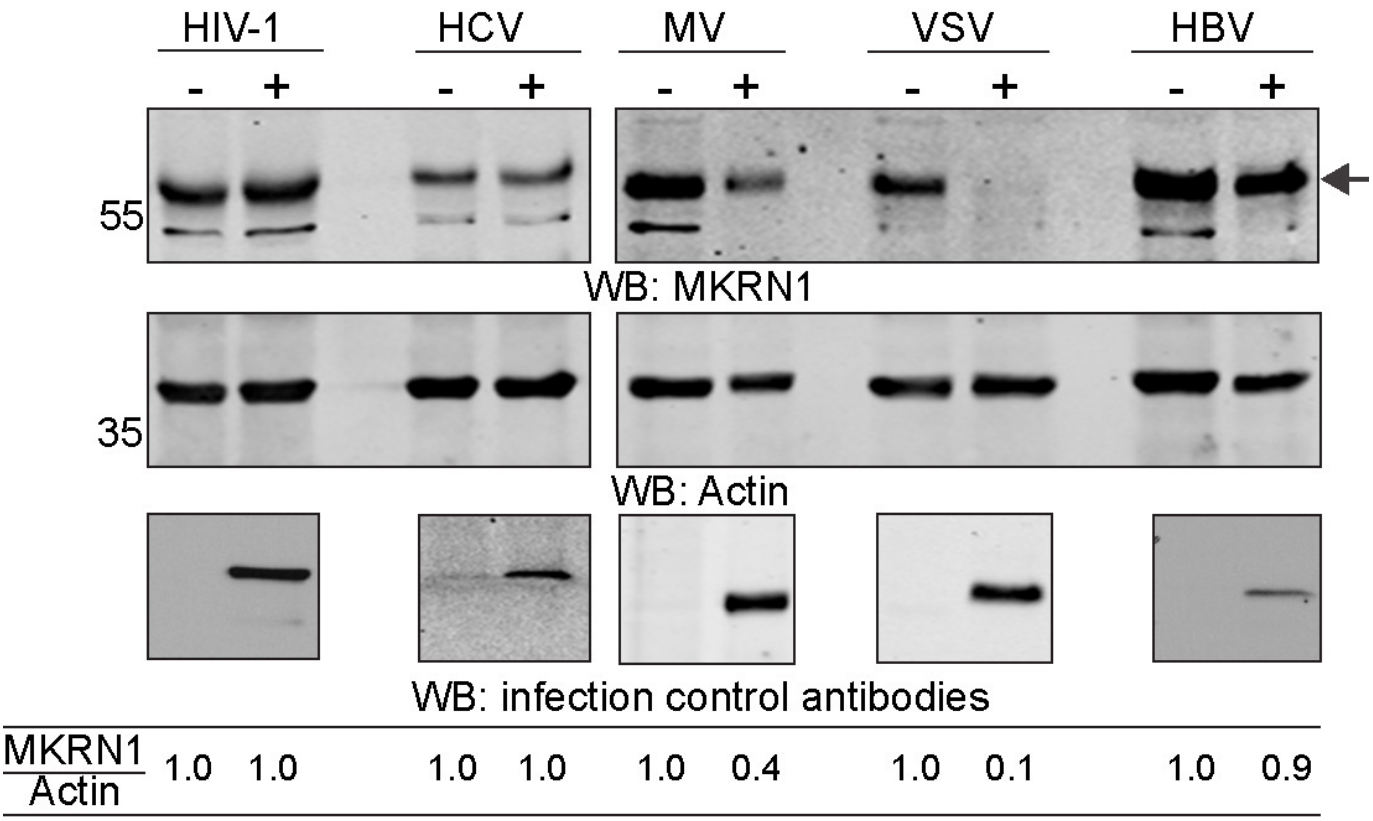

MKRN1 / Actin	1.0	1.0	1.0	1.0	1.0	0.4	1.0	0.1	1.0	0.9